Colloids and Surfaces B: Biointerfaces 75 (2010) 432–440

Contents lists available at ScienceDirect

Colloids and Surfaces B: Biointerfaces

journal homepage: www.elsevier.com/locate/colsurfb

Tat peptide mediated cellular uptake of SiO_2 submicron particles

Zhengwei Mao, Li Wan, Ling Hu, Lie Ma, Changyou Gao*

Key Laboratory of Macromolecular Synthesis and Functionalization, Ministry of Education, and Department of Polymer Science and Engineering, Zhejiang University, Hangzhou 310027, China

ARTICLE INFO

Article history:
Received 20 June 2009
Received in revised form 16 August 2009
Accepted 15 September 2009
Available online 2 October 2009

Keywords:
Cell uptake
Subcellular distribution
Tat
Silicon dioxide
Particles

ABSTRACT

Internalization of nano- and microparticles into live cells correlates closely with their potential applications, functions, cytotoxicity and intracellular drug delivery. Particularly, delivery of a large variety of cargoes such as proteins, peptides, nucleic acids and small particles into cells could be enhanced by some ligands such as Tat peptide. In this work, the ability of Tat mediated cellular uptake was assessed. The Tat peptide was covalently immobilized to fluorescein tagged SiO_2 particles (FITC–SiO_2–NH_2 particles) with a diameter of 200 nm. BCA protein assay determined that the grafting amount of the Tat peptide could be controlled within a range of 0–3.5 μg/mg SiO_2 particles by the Tat feeding amount. Surface immobilization of the Tat peptide did not bring apparent changes on the surface morphology and charge property of the SiO_2–NH_2 particles. By contrast, the surface charge of both the FITC–SiO_2–NH_2 particles and the FITC–SiO_2–Tat particles was reversed from slight positive in Dulbecco's Modified Eagles Medium (DMEM) to slight negative in DMEM/fetal bovine serum, conveying adsorption of plasma proteins on the particles. Flow cytometry measurement showed that the FITC–SiO_2–Tat particles were internalized by HepG2 cells with a significant faster rate and a higher number of particles than that of the FITC–SiO_2–NH_2 particles. Moreover, internalization of the Tat peptide decorated particles was less influenced by the low temperature at 4 °C. The Tat decoration affected the subcellular distribution of the particles as well, resulting in localization of the particles in the cell nucleus. No obvious cytotoxicity was detected for both the FITC–SiO_2–NH_2 particles and the FITC–SiO_2–Tat particles.

1. Introduction

With significant developments in the understanding of colloidal particle (characterized by a length scale ranging from 1 nm to microns) systems, research efforts are being focused on integrating them with biology [1]. In particular, the colloidal particles have shown great potentials in diagnostics, biosensing, and therapeutics. So far, several colloidal particle systems have been used to deliver chemotherapeutic agents to specific sites, which can minimize the toxic effects on healthy tissues while sustain the drug release profile [2]. For example, the use of silica or silicon dioxide particles in the biomedical field has been progressing for several years with a main focus on cell recognition for diagnostics as well as drug and gene delivery [3–7]. In those cases where the colloidal particles are utilized as medication carriers, the drugs are generally adsorbed or covalently linked onto the surfaces of the particles. The drug release mechanisms are triggered by simple desorption kinetics or degradation of the covalent linkages between the drug molecules and particle surfaces. One major advantage of the silica and silicon dioxide particles is that they are deemed toxicologically safe because of their high stability, which has been proven in 50 years of use as a pharmaceutical excipient for oral drug delivery [8].

As the field continues to develop, qualitative and quantitative studies on cellular uptake of the colloidal particles with respect to their physical and chemical parameters are urgently required. One pathway for the colloid internalization is known as phagocytosis or endocytosis [9]. As the phagocytosis generally involves the uptake of particles larger than 500 nm, the colloids with a smaller size are thought to be mainly endocytosized. For example, the PLGA nanoparticles were found to be ingested by cells via endocytosis [10,11]. During the endocytosis process, the colloids are gradually embedded by invagination of the membrane and endocytosized into the cell. A portion of the plasma membrane is invaginated and pinched off, forming membrane-bounded vesicles called endosomes. The endosomes then deliver their contents to lysosomes. The membranes of the two organelles fuse. Once inside the lysosomes, the ingested colloids are destroyed by the degradative enzymes or repelled out of the cell.

The endocytosis may be a receptor-mediated or non-receptor-mediated process [12]. The important parameters controlling the cell–particle interaction include particle size, shape, surface

* Corresponding author. Tel.: +86 571 87951108; fax: +86 571 87951108.
E-mail address: cygao@mail.hz.zj.cn (C. Gao).

0927-7765/$ – see front matter © 2009 Elsevier B.V. All rights reserved.
doi:10.1016/j.colsurfb.2009.09.017

chemistry and surface charge [13–15]. For example, Chithrani and Chan found that the gold nanoparticles with a diameter of ~50 nm were taken up by mammalian cells with a faster rate and higher concentration than that with other sizes and shapes [16]. Our results showed that the SiO_2 particles with a diameter of ~200 nm were taken up by HepG2 cells with a faster rate and higher concentration than that of other sizes. Champion and Mitragotri also showed that the shape of micrometer-sized polystyrene particles mediated their uptake in alveolar macrophages [17]. Chemical characteristics such as surface charge may determine the fate of the nanoparticles in cells. Mailänder and co-workers demonstrated that uptake of the submicron-sized polymeric particles by HeLa cells and human mesenchymal stem cells (MSCs) was enhanced by functionalizing their surface with cationic groups [18]. Huang et al. also showed that the positively charged surface could enhance the uptake of silica nanoparticles in human MSCs [19]. Moreover, escape of the particles from the endosomes into the cellular cytoplasm was regarded as a result of a change of surface charge from negative to positive, resulting in cytoplasmic delivery of the incorporated drugs [10,11].

Immobilization of a cell binding receptor on the particle surface is another effective method to enhance their cellular uptake. For example, Prasad and co-workers synthesized the folate conjugated quantum dots and demonstrated the receptor-mediated delivery of the quantum dots into folate receptor positive cell lines [20]. This is an important area of the targeted entry into cells [13,14]. The nucleus is a desirable target because the genetic information of the cell and transcription machinery resides there. Targeted nuclear delivery is a challenging task because a nuclear probe must, at least, satisfy the requirements of (1) being internalized into the cell (e.g. through receptor-mediated endocytosis), (2) escaping from the endosomal pathways, (3) having a nucleus localization signal to interact with the nuclear-core complex, and being able to cross the nuclear membrane [15]. The most efficient nuclear targets in biology are viruses, which commonly utilize different proteins for crossing each cell membrane barrier. Artificial systems having the model viral behaviors could be designed on derivatives of functionalized nanoparticles to induce cell entry and nucleus targeting [21].

Over the last decade, several publications revealed a massive improvement in the cellular delivery of various biologically active molecules upon their attachment to a peptide derived from the HIV-1 Tat protein [22]. This peptide encompasses a highly cationic cluster composed of 6 arginine and 2 lysine residues in the very middle of the peptide sequence [23]. The 'transduction domain' or region conveying the cell penetrating properties appears to be confined to a small (9 amino acids) fragment of basic amino acids, with the sequence of RKKRRQRRR [24–27]. This artificially synthesized peptide analogue with biological activities was named as Tat peptide, which has been shown great success in delivering a large variety of cargoes, from small particles to proteins, peptides and nucleic acids [28–31]. For example, Au NPs (20 nm) were covered with shells of bovine serum albumin (BSA), which were conjugated to Tat and other cellular targeting peptides. The functional nanoparticles could penetrate the biological membrane and target the nucleus [14]. Moreover, A Tat peptide-based micelle delivery system has been developed [32], in which not only the translocation of the micelles into the cells was accelerated but also their location on the nucleus envelopes was enhanced. It was also demonstrated that the Tat peptide can mediate delivery of nanoparticles (70 nm) to mouse brain in vivo without compromising the blood brain barrier [33].

So far, we have prepared various hollow structures including polymeric capsules and SiO_2 hollow spheres, whose size ranges from submicron to a few microns [34,35]. These hollow structures can be used as drug and gene carriers for various applications, including the intracellular therapy. For this purpose, the surface chemistry of the particles is extremely important, which is decisive to the cellular uptake and intracellular delivery. Although the Tat peptide has been proven to be an effective molecule to induce cell uptake of nanosized molecules or particles (<100 nm), their effect on relative large particles (with the diameter between 100 nm and 1000 nm), which are also very useful in drug delivery, has rarely been studied. Only Fretz et al. [36] coupled the Tat peptide to the liposome surface (~200 nm), and found the enhanced cellular uptake of liposomes via the endocytosis pathway. Although Santra et al. have demonstrated that the Tat conjugated fluorescent silica nanoparticles with a size of 70 nm are rather promising for bioimaging, the cellular distribution which is very important for the eventual fate and potential applications of the colloidal particles has not been studied [33]. Moreover, the coupling reagent (*N*-succinimidyl 3-(2-pyridyldithio)propionate) is rather expensive. In this work, effect of the Tat peptide grafted on submicron particles (via a low-cost and convenient pathway), exemplified as the SiO_2 particles for their stable physical and chemical structures, shall be studied in terms of the cellular penetration and potential of nucleus targeting. Particle distribution within the cells and cytotoxicity shall also be evaluated.

2. Materials and methods

2.1. Materials

Fluorescein isothiocyanate (FITC) was purchased from Sigma–Aldrich. Tat peptide (H-Tyr-Gly-Arg-Lys-Lys-Arg-Arg-Gln-Arg-Arg-Arg-OH, Mw = 1559) was purchased from Bachem AG, Germany. Enhanced BCA protein assay kit was purchased from Beyotime Biotechnology Inc., Nantong, China. Ethidium bromide (EB) was purchased from Fluka. All other reagents were of analytical grade and used as received. Double-distilled water was used throughout the study. Human liver cancer cells (HepG2) were maintained in Dulbecco's Modified Eagles Medium (DMEM, Gibco) supplemented with 100 U/ml penicillin, 100 μg/ml streptomycin and 10% fetal bovine serum (FBS, Sijiqing Co. Ltd., Hangzhou, China). The cells were incubated at 37 °C in a humidified atmosphere containing 5% CO_2 and used at an appropriate degree of confluence.

2.2. Particle preparation

FITC-modified triethoxysilane was prepared from (3-aminopropyl)triethoxysilane (APS) and FITC under nitrogen flow using a standard Schlenk line technique [37–40]. A mixture of 0.3 ml tetraethyl orthosilicate (TEOS) and 1 ml FITC-modified APS (TEOS/FITC-APS with a molar ratio of 0.3/0.04) was injected into the mixture of 37.2 ml ethanol and 20.5 ml water. Polymerization was initiated by ammonia solution (6 ml, 30 wt% of $NH_3 \cdot H_2O$). Another 2.7 ml TEOS was added into the flask after 1 h. 5 h later, one third of the reaction product was centrifuged at 10,000 × *g* for 10 min to obtain the silicon dioxide particles containing the organic dye (FITC–SiO_2). The remained two third reaction product was further reacted with 0.2 ml APS at room temperature for 2 h in a N_2 atmosphere to obtain the aminosilanized SiO_2 particles (FITC–SiO_2–NH_2). The FITC–SiO_2–NH_2 particles were isolated from the unreacted Si compounds by centrifugation and washing with ethanol for 5 times. Briefly, the FITC–SiO_2–NH_2 were mixed with ethanol and separated by centrifugation at 13,000 rpm for 20 min. After the supernatant was discarded, fresh ethanol was added. The precipitated particles were redispersed by sonication for 20 min. Finally, the FITC–SiO_2–NH_2 particles were freeze-dried and stored in dark.

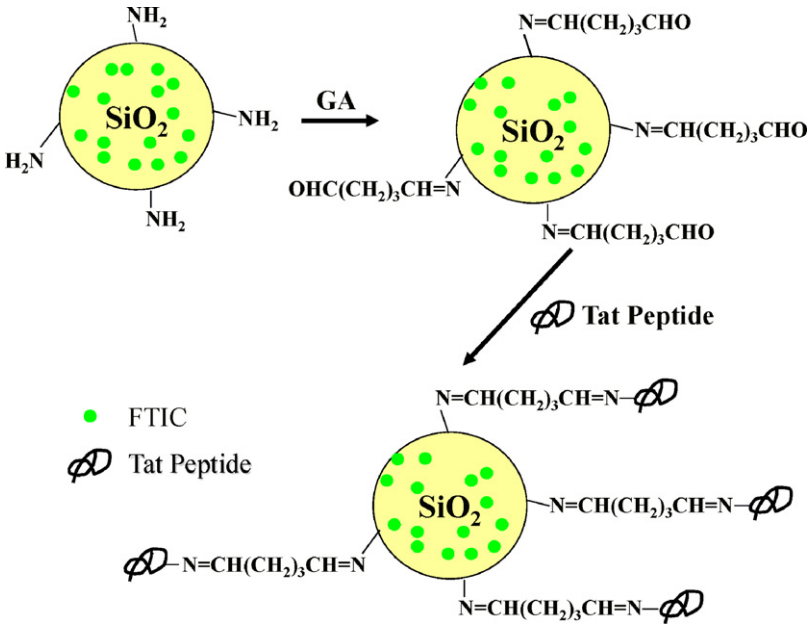

Scheme 1. The schematic representation to show the production process of Tat modified FITC–SiO_2 particles.

2.3. Grafting Tat peptide onto the SiO_2–NH_2 surface

The procedures for Tat peptide grafting onto the FITC–SiO_2–NH_2 particles are shown in Scheme 1. 10 mg FITC–SiO_2–NH_2 particles were dispersed in 1 ml 5% glutaraldehyde (GA) solution. The reaction was carried out at 4 °C overnight to convert the –NH_2 groups into –CHO groups, yielding aldehyde enriched FITC–SiO_2 particles (FITC–SiO_2–CHO). The FITC–SiO_2–CHO particles were centrifuged and washed with phosphate buffered saline (PBS) 5 times to remove the unreacted GA. As some particles were inevitably lost during this process, concentration of the FITC–SiO_2–CHO particles was adjusted by fluorophotometer (LS55, PerkinElmer, U.K.) with a final concentration of 5 mg/ml. The Tat peptide was dissolved in PBS with a final concentration of 1 mg/ml. 5 mg FITC–SiO_2–CHO particles were mixed with a desired volume of Tat peptide solution to covalently graft the Tat peptide (FITC–SiO_2–Tat). After the reaction was carried out at 4 °C overnight, 1 ml 5 mg/ml lysine solution was used to terminate the unreacted aldehyde groups. The FITC–SiO_2–Tat particles were centrifuged and washed with PBS 5 times to remove the unreacted Tat peptide. Finally, the FITC–SiO_2–Tat particles were freeze-dried and stored at −20 °C in dark.

2.4. Quantification of the grafting amount of the Tat

The BCA method using bicinchoninic acid (BCA) is very effective and sensitive to determine the minor amount of surface immobilized proteins. In this analysis, Cu^{2+} ions are reduced to Cu^{+} ions by the proteins or peptides. One Cu^{+} ion combines with 2 BCA molecules to give a purple colored complex which exhibits a strong absorbance at 562 nm. The reaction can proceed regardless of the state of proteins, i.e. free and immobilized [41]. The FITC–SiO_2–Tat particles were dispersed in PBS with a final concentration of 50 mg/ml. 20 μl particle suspension was added to 200 μl BCA test solution. After the reaction was performed at 37 °C for 30 min, the mixture solution was centrifuged at 20,000 × *g* for 10 min. The absorbance of the supernatant was measured by a microplate reader (model 550, Bio-Rad) at a wavelength of 570 nm. The Tat amount was obtained by referring to a calibration curve recorded from a series concentration of Tat peptide solution at the same conditions.

2.5. Characterization

The morphology of the FITC–SiO_2–NH_2 and FITC–SiO_2–Tat particles was observed using a JEOL JEM-200 transmission electron microscope (TEM). Briefly, a drop of the particle suspension was applied onto carbon-coated grids and dried at 25 °C, and then were observed.

The zeta potential measurements were performed using an aqueous dip cell in the automatic mode (Zetasizer 3000, Malvern Instruments, Southborough, MA). The particle suspension was mixed with equal volume of 2× DMEM solution and 2× DMEM/20% FBS (fetal bovine serum) solution, resulting in a normal particle containing DMEM solution and DMEM/10% FBS solution, respectively. The pH value of the solution was adjusted to 7.4.

2.6. Cellular uptake of the particles

HepG2 cells were seeded onto a 24-well plate (Corning, New York, USA) at a density of 1×10^5 cells per well in 1 ml culture medium (DMEM containing 10% FBS, supplemented with 100 U/ml of penicillin and 100 μg/ml of streptomycin). The particles with a final concentration of 40 μg/ml were cocultured with the cells at either 37 °C or 4 °C. At determined time intervals, the cells were carefully washed 3 times with PBS, and then were trypsinized and resuspended in the medium. The fluorescence intensity of the cells was analyzed by a FACSCalibur flow cytometry (BD Bioscience). Untreated HepG2 cells were used as a negative control.

To monitor the cellular uptake of the SiO_2 particles, all the cells were cultured on glass slides (the slides were pre-laid on the well bottoms of a 24-well culture plate) with the presence of 40 μg/ml particles at 37 °C. At determined time intervals, the cells were carefully washed 3 times with PBS, and then fixed by 1% formaldehyde in PBS at room temperature for 15 min. After carefully washed 3 times with PBS, the cells were stained by 100 μg/ml EB solution in PBS for 10 min. After washed 3 times with PBS, the cells were observed by confocal laser scanning microscopy (CLSM, Bio-Rad 2100). The section was focused on the middle of the cells with a thickness smaller than 0.7 μm.

To observe the cell morphology by scanning electron microscopy (SEM), the cells were washed with PBS and fixed with

2.5% glutaraldehyde in PBS at 4 °C for 48 h after cocultured with the SiO_2 particles for 24 h. After washed with PBS to remove the GA, the cells were dehydrated with a graded series of ethanol, and then were dehydrated with acetone and isoamyl acetate. After dried by the critical point dry method, the cells were coated with an ultrathin gold layer and observed under SEM (Cambridge stereoscan 260 and FEI SIRION-100).

2.7. Toxicity of the particles

200 μl HepG2 cell suspension was seeded in a well of 96-well polystyrene plate, with a final cell number of 1×10^4/well. After 24 h, 20 μl particle suspension was added into the culture medium with a final concentration of 40 μg/ml. The culture medium containing the same concentration of SiO_2 particles was changed every 2 days. The cell proliferation was measured using a methylthiazoletetrazolium (MTT) method [42]. The absorbance was recorded at a wavelength of 570 nm by a microplate reader (model 550, Bio-Rad). Three parallel experiments were conducted.

2.8. Statistical analysis

Data are expressed as the mean ± standard deviation (SD), $n = 3$ if not specially mentioned. Statistical analysis was performed using the two population Student's t-test. The significant level was set as $P < 0.05$.

3. Results and discussion

3.1. Characterization of FITC–SiO_2–Tat particles

Following the synthesis procedures shown in Scheme 1, FITC–SiO_2–Tat particles were obtained, and the Tat amount immobilized on which was characterized by BCA protein assay kit. Along with increase of the feeding Tat amount, linear increase of the Tat peptide on the particles was found until the feeding Tat amount reached to 5 μg/mg FITC–SiO_2 particles (Fig. 1), at which the immobilized Tat amount was 3.5 μg/mg FITC–SiO_2 particles. Above this feeding amount the immobilized Tat amount was not changed. This alteration behavior is quite reasonable since the –CHO numbers on each particle are definite. The saturation at 3.5 μg/mg implies that all the available –CHO groups may have been reacted with the Tat peptide. Taking into account the particle diameter (200 nm) and SiO_2 density (2 g/cm^3), 3.5 μg/mg Tat equals to 10^4 Tat molecules per SiO_2 particle, namely 1 Tat molecule per 12 nm^2 surface, conveying a quite high grafting density. For brevity, in the following study the particles having the Tat amount of 2 μg/mg and 3.5 μg/mg are designated as FITC–SiO_2–Tat2 and FITC–SiO_2–Tat3.5, respectively.

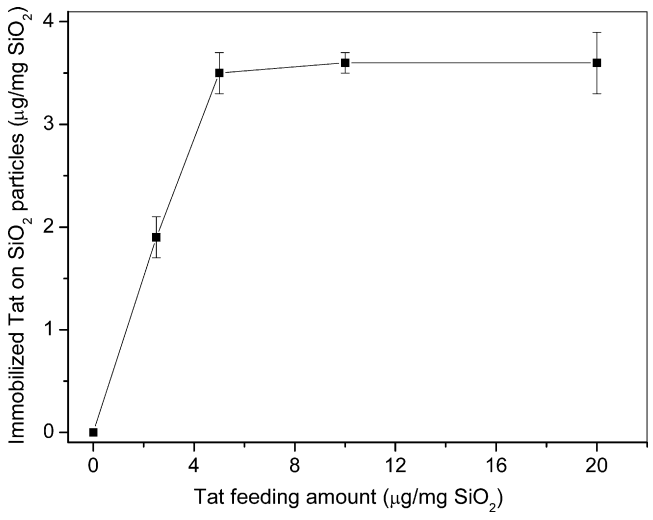

Fig. 1. Immobilized Tat amount on FITC–SiO_2 particles as a function of feeding Tat amount.

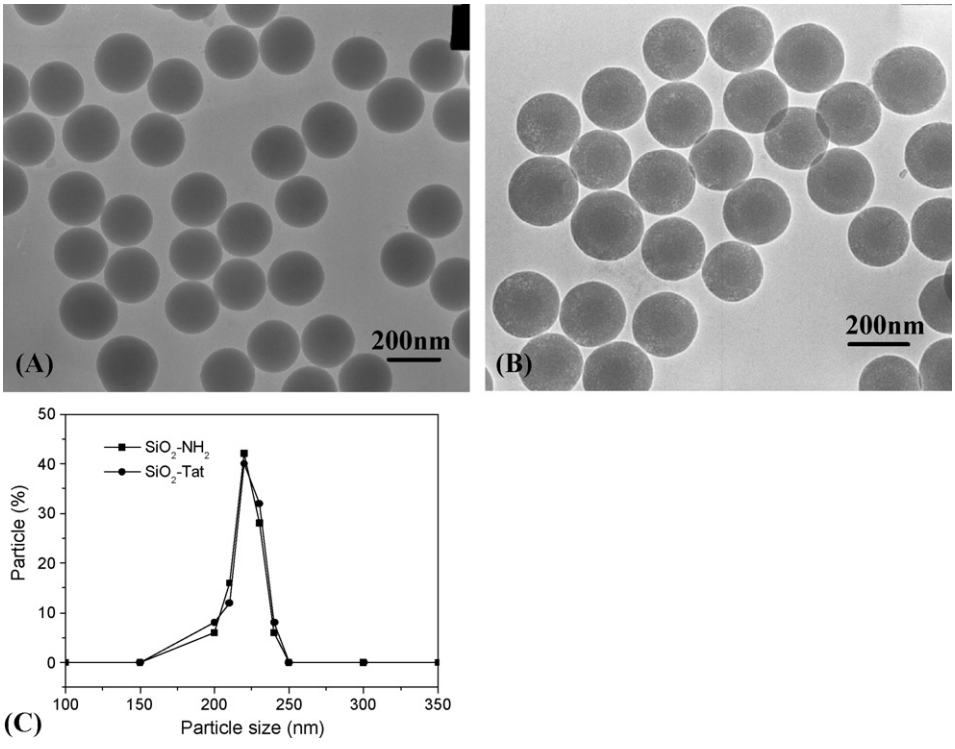

Fig. 2. TEM images of (A) FITC–SiO_2–NH_2 particles and (B) FITC–SiO_2–Tat3.5 particles. (C) The size histogram of FITC–SiO_2–NH_2 and FITC–SiO_2–Tat3.5 particles obtained from the TEM images.

Fig. 2 presents the representative TEM images of the FITC–SiO_2–NH_2 (Fig. 2A) and FITC–SiO_2–Tat3.5 (Fig. 2B) particles. The majority of the FITC–SiO_2–Tat3.5 and FITC–SiO_2–NH_2 particles are uniform spherical, with a diameter of ~200 nm. No obvious difference could be found in terms of the particle shape, size and dispersion (Fig. 2C) by TEM after Tat peptide grafting.

The surface charge of the particles is very important for the cellular internalization. Positively charged particles can electrostatically adsorb on the negatively charged cell membrane, and then clathrin-dependent or receptor induced endocytosis is responsible for the cellular uptake of the particles [43]. Due to the weak positively charged nature of the Tat peptide (eight amino group residues in one peptide molecule), both its grafting density and environmental conditions might influence the surface charge density of the resultant particles. Therefore, their zeta potentials were measured in DMEM and DMEM/10% FBS media, in which the cells were cultured. Fig. 3 shows that in both DMEM and DMEM/FBS media the zeta potential of the FITC–SiO_2–Tat particles kept almost unchanged after Tat immobilization. Compared to the positive surface charge in DMEM, the surface charge of the FITC–SiO_2–Tat particles and the FITC–SiO_2–NH_2 particles

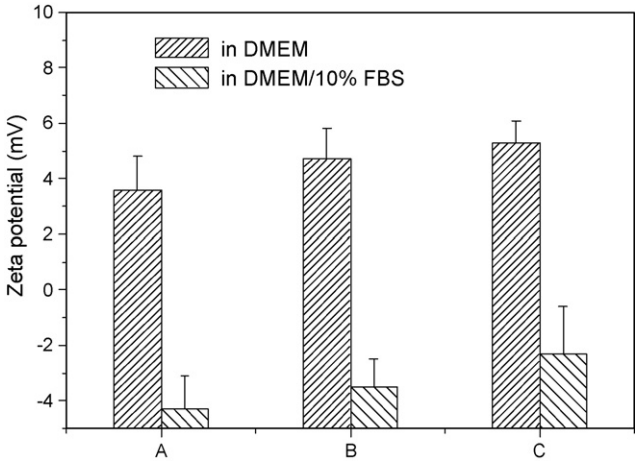

Fig. 3. Effect of Tat immobilization amount on the zeta potentials of FITC–SiO_2 particles. (A) FITC–SiO_2–NH_2 particles, (B) FITC–SiO_2–Tat2 particles and (C) FITC–SiO_2–Tat3.5 particles. The measurements were carried out in DMEM and DMEM containing 10% FBS, respectively.

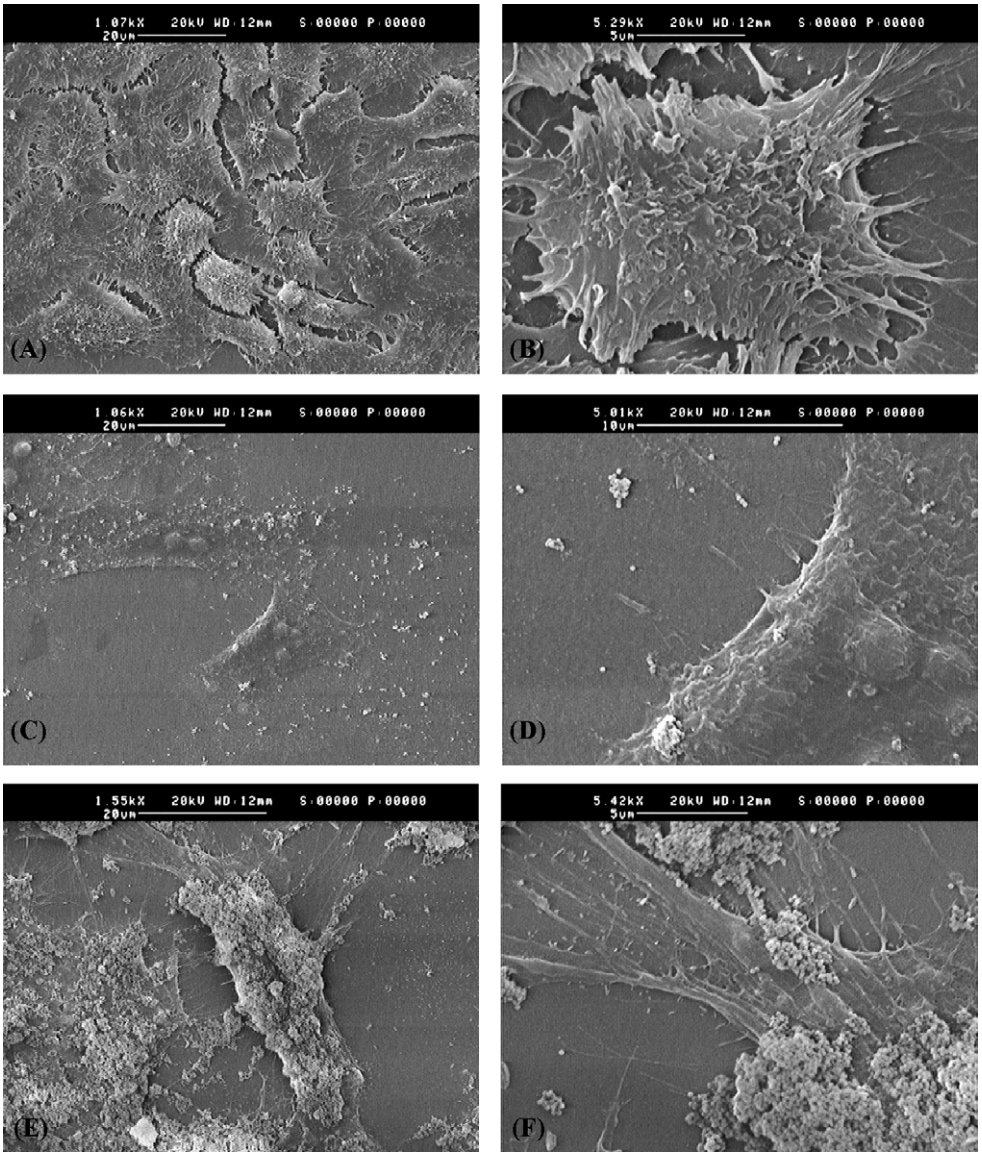

Fig. 4. The morphology of HepG2 cells observed by SEM after in vitro cultured for 24 h. (A) particles free control, (C) cocultured with FITC–SiO_2–NH_2 particles, and (E) cocultured with FITC–SiO_2–Tat3.5 particles. (B), (D) and (F) are higher magnification of the (A), (C) and (E), respectively.

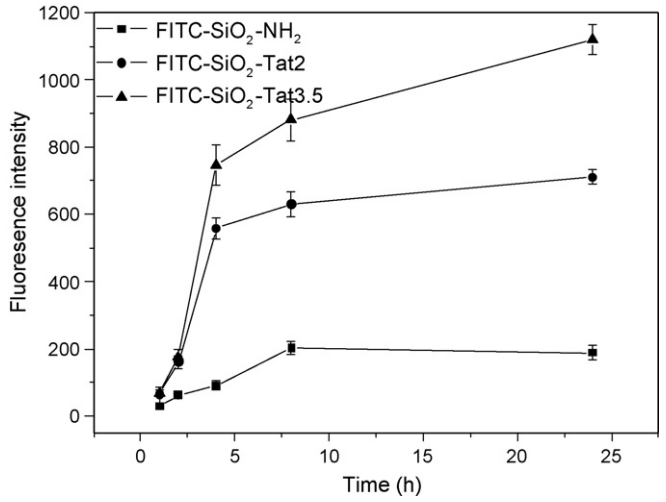

Fig. 5. Fluorescence intensity per cell as a function of incubation time. FITC–SiO_2–NH_2, FITC–SiO_2–Tat2 and FITC–SiO_2–Tat3.5 particles (40 μg/ml) were incubated with HepG2 cells in DMEM/10% FBS at 37 °C.

was reversed into negative in DMEM/FBS. This charge reversal is understood as the result of adsorption of the serum proteins, which are negatively charged at physiological conditions. Nevertheless, the zeta potentials of the FITC–SiO_2–Tat particles and the FITC–SiO_2–NH_2 particles in the same medium are not significantly different (for the FITC–SiO_2–Tat3.5 and FITC–SiO_2–NH_2 particles, $P < 0.05$ in DMEM but $P = 0.17$ in DMEM/10% FBS), so that the surface charge influence on the cellular uptake can be safely ruled out.

3.2. Cell morphology observed by SEM

The cell–particle interaction was firstly subject to SEM investigation (Fig. 4). Only a very few FITC–SiO_2–NH_2 particles (Fig. 4C and D) attached to the HepG2 cell surface after cocultured for 24 h, with no obvious cell morphology change compared with the particles free control (Fig. 4A and B). On the other hand, the cells cocultured with the FITC–SiO_2–Tat3.5 particles (Fig. 4E and F) showed different appearance. A large number of particles attached onto the cell membranes in a format of clusters, covering almost the whole cells. However, no obvious change of the filopodia and lamellipodia as well as the cytoskeleton was observed. One can conclude that the Tat peptide coating can significantly enhance the attachment of the SiO_2 particles on the cell membrane without disturbing cell morphology.

3.3. The internalization of SiO_2 particle

In the next study, internalization of the SiO_2 particles with and without Tat peptide immobilization was monitored as a function of culture time. As shown in Fig. 5, the fluorescence intensity recorded from the cells was very weak after in vitro culture for 1 h, indicating that very few FITC–SiO_2–NH_2 particles, regardless the Tat decoration, were adsorbed on the cell membranes or uptaken by the cells. During the next 7 h, the fluorescence intensity was increased rapidly. After that, the FITC–SiO_2–NH_2 group reached a plateau, while slight increase was still found for the FITC–SiO_2–Tat groups. At the same culture time except for the first hour, the FITC–SiO_2–Tat groups always had the significant stronger fluorescence intensity ($P < 0.01$) than that of the FITC–SiO_2–NH_2 group. At the initial stage before 8 h, more sharp increase of the fluorescence intensity was found for the FITC–SiO_2–Tat groups, especially the one with larger Tat peptide amount. These results confirm that the FITC–SiO_2–Tat particles have a faster cellular uptake rate than that of the FITC–SiO_2–NH_2 particles, implying a different uptake pathway. Quantitative analysis showed that at 8 h the average fluorescence intensity per cell from the FITC–SiO_2–Tat2 group and FITC–SiO_2–Tat3.5 group was 3 times and 4.5 times higher than that from the FITC–SiO_2–NH_2 group, respectively. Thus, the results confirm further that with more Tat peptide on the particles, a larger number of particles is internalized at the same culture time, while the bare FITC–SiO_2–NH_2 particles has the weakest ability to be internalized. It is worth noting that the FCM methodology in this study analyzes the overall fluorescent signal of the cells, which cannot distinguish if the signal is originated from the cell membranes or from the cell interiors.

Although the function of the Tat peptide for delivering cargoes into the cells has been identified, so far the mechanism of internalization of Tat peptide is unclear. There appears to be two kinds of mechanisms involved, depending upon the size of the cargos. Smaller molecules attached to Tat seem to transduce directly into the cells by the energy independent electrostatic interaction and hydrogen bonding [45], but larger cargos get into the cells by an energy dependent macropinocytosis pathway [44]. To further study the mechanism of the Tat induced particles internalization, the uptake experiments were carried out at 37 °C and 4 °C for 4 h, respectively. As shown in Fig. 6, the fluorescence intensity of the FITC–SiO_2–NH_2 group was decreased to 17.4% at 4 °C of that at 37 °C, while the fluorescence intensity of the FITC–SiO_2–Tat3.5 group was only decreased to 54.8% at 4 °C of that at 37 °C. This result reveals that the internalization of the FITC–SiO_2–NH_2 and FITC–SiO_2–Tat3.5 particles is via the endocytosis way, which is dramatically blocked at low temperature during this time window. Yet the internalization of the Tat peptide decorated particles is less influenced by the temperature decrease, indicating a different internalization pathway. As the zeta potential of the FITC–SiO_2–Tat3.5 particles is almost identical to that of the FITC–SiO_2–NH_2 particles in DMEM/FBS (Fig. 3), the intrinsic force might be the affinity between the Tat peptide and the cell membrane [46,47], suggesting a receptor-mediated uptake mechanism. Unfortunately, there still a mystery what is the exact interaction between the Tat peptide and the cell membrane.

To identify the particle localization inside the cells, CLSM images of the HepG2 cells were taken as a function of time (Fig. 7). The images were taken in the middle of the cells with a section thickness of about 0.7 μm, which guarantees all the signals are collected from inside of cells since normally a cell has a thickness over several micrometers. At the first 3 h, the bare FITC–SiO_2–NH_2 particles were

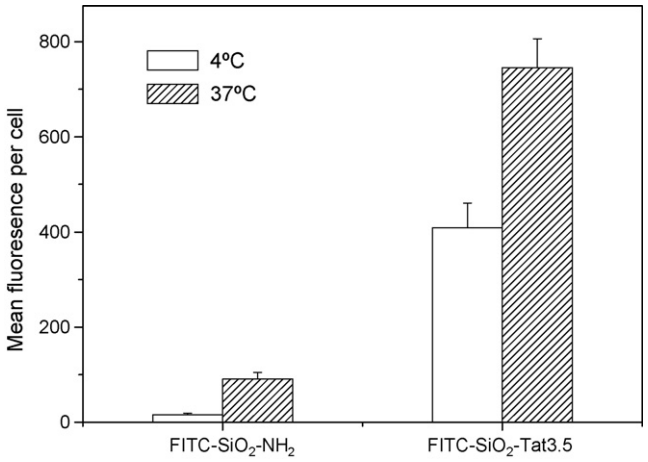

Fig. 6. Fluorescence intensity per cell of HepG2 cells incubated with FITC–SiO_2–NH_2 and FITC–SiO_2–Tat particles (40 μg/ml) in DMEM/10% FBS at 4 °C and 37 °C for 4 h, respectively.

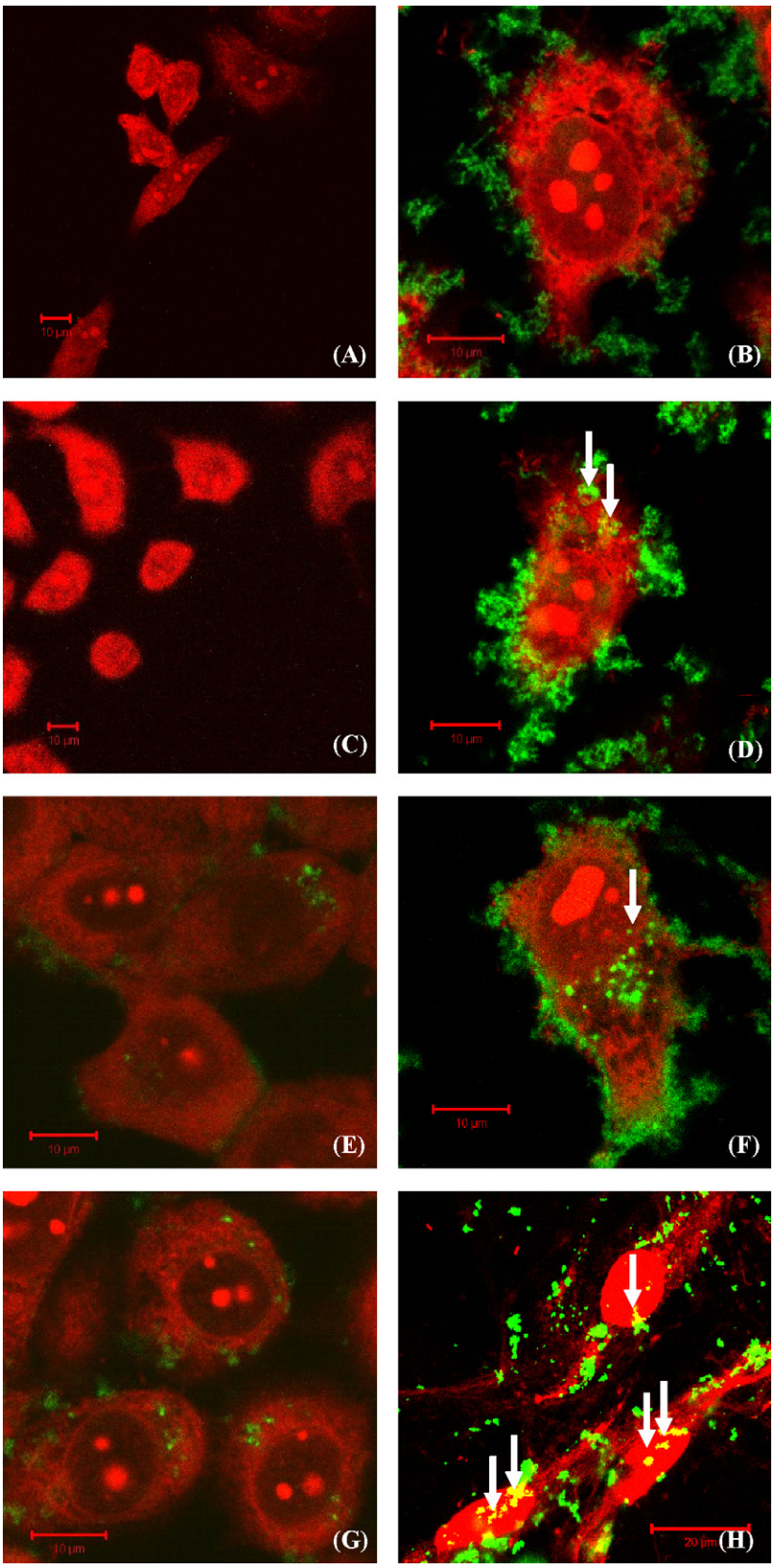

Fig. 7. Cellular distributions of FITC–SiO_2–NH_2 and FITC–SiO_2–Tat3.5 particles as a function of incubation time. HepG2 cells (labeled with EB to show red color) incubated with FITC-labeled SiO_2 particles (40 μg/ml). (A), (C), (E) and (G) FITC–SiO_2–NH_2 particles incubated for 1 h, 3 h, 6 h and 24 h, respectively, and (B), (D), (F) and (H) FITC–SiO_2–Tat3.5 particles incubated for 1 h, 3 h, 6 h and 24 h, respectively. The slice thickness is <0.7 μm. The Images were recorded at the equatorial planes in *Z*-direction of the cells. Bar is 10 μm.

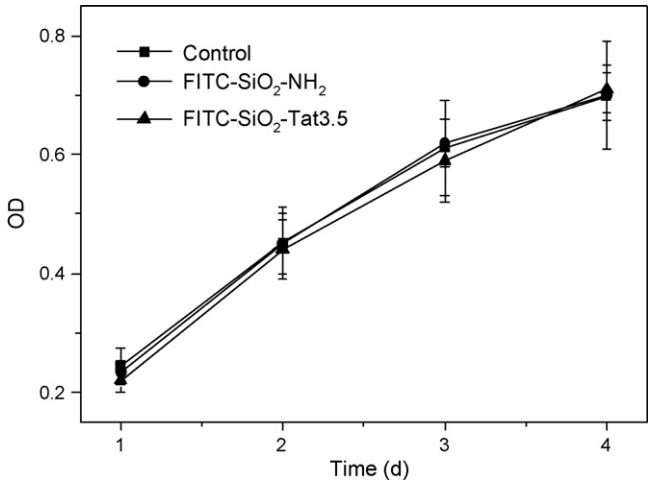

Fig. 8. HepG2 cells' viability as a function of culture time in the presence of FITC–SiO_2–NH_2 and FITC–SiO_2–Tat3.5 particles, respectively.

hardly found on the cell membranes and inside the cell cytoplasms (Fig. 7A and C). This result is consistent with the data of FCM test, in which the fluorescence intensity per cell was quite low at the first 4 h (Fig. 5). Until cocultured with the cells for 6 h (Fig. 7E), a few particles were observed on the cell membranes and inside the cells. The particle amount inside the cells was increased after 24 h coculture (Fig. 7G). Even at this time, only one or two particles were found on a nuclear envelope, but no particle was found inside the nucleus.

For the FITC–SiO_2–Tat3.5 particles, a lot of particles were already found on the cell membranes (Fig. 7B) after 1 h cocultured. After 3 h (Fig. 7D), more particles were adsorbed onto the cell membranes, and some particles were aggregated in the cytoplasm (arrow headed, most possibly in the endosomes or lysosomes) of the cell. After 6 h, some particles attached on the nucleic envelope (Fig. 7F), with one even inside the nucleus (arrow indicated), implying that the particles may penetrate the nucleic envelope. After 24 h coculture, a lot of FITC–SiO_2–Tat3.5 particles could be found inside the nucleus (Fig. 7H, arrows headed), forming particle clusters. Unfortunately, the trial to further prove the nucleus location of particles via TEM was failed because too many particles located on/inside cells making them very difficult to section. Nevertheless, the result from CLSM still can indicate that the Tat peptide can mediate entrance of large particles (200 nm in diameter) into the cell nucleus, conveying some promising applications for nucleus delivery, for example, gene therapy. The mechanism of Tat mediated nucleus penetration is unclear. The particles (200 nm) are too large to penetrate the nucleus pores (~30 nm). In this sense, the penetration process might be related to the nucleus duplication and cell proliferation [48]. Since nuclear envelope breakdowns during the mitosis process, the particles in cytoplasm have a chance to diffuse into nucleoplasm and stay inside nucleus after the recreation of nuclear envelope.

3.4. Toxicity of SiO_2 particles

The cytotoxicity of the FITC–SiO_2–Tat3.5 and the FITC–SiO_2–NH_2 particles was tested using MTT assay. The cell viability was proportional to the OD value by measuring conversion of the MTT tetrazolium compound to formazan. For both kinds of the particles (Fig. 8), the cell viability was comparable to the particle free control sample during the 4 days' culture, indicating that the particle internalization with the present dose has no side effect on the cell proliferation regardless of the Tat peptide decoration. The normal proliferation of the cells could then bring the particles in the nucleus as discussed above (Fig. 7).

4. Conclusion

The Tat peptide was covalently immobilized onto the fluorescein tagged SiO_2 (FITC–SiO_2–NH_2) microparticles with a diameter of 200 nm. The immobilized amount of the Tat peptide was initially increased along with the feeding Tat amount until 5 μg/mg SiO_2 particles, at which 3.5 μg was immobilized onto 1 mg SiO_2 particles. This value equals to 10^4 Tat molecules per SiO_2 particle, namely 1 Tat molecule per 12 nm^2 surface. No obvious change on the morphology and zeta potential of the particles has been observed after Tat immobilization. Both the cell uptake rate and the final uptake amount of the SiO_2 particles were significantly improved by surface Tat decoration. Moreover, compared to the FITC–SiO_2–NH_2 particles the cellular uptake of the FITC–SiO_2–Tat particles was less influenced by low temperature, indicating receptor-mediated internalization mechanism. Confocal microscopy revealed also that the FITC–SiO_2–Tat particles were capable of localization in the cell nucleus after in vitro culture for 24 h. No obvious cytotoxicity was detected for both the FITC–SiO_2–NH_2 particles and the FITC–SiO_2–Tat particles. The results demonstrate that the Tat peptide can effectively delivery considerable large cargos into cells and even into cell nucleus, with less influence by temperature alteration. By making use of this feature, improvement of the intracellular delivery of colloidal carriers for drugs and genes can be envisaged.

Acknowledgements

This study is financially supported by the National Science Foundation of China (No. 50873087) and the Major State Basic Research Program of China (No. 2005CB623902).

References

[1] A. Anshup, J.S. Venkataraman, C. Subramaniam, R.R. Kumar, S. Priya, T.R. Kumar, R.V. Omkumar, A. John, T. Pradeep, Langmuir 21 (2005) 11562.
[2] W.T. Liu, J. Biosci. Bioeng. 102 (2006) 1.
[3] I. Roy, T.Y. Ohulchanskyy, D.J. Bharali, H.E. Pudavar, R.A. Mistretta, N. Kaur, H. Pudavar, P.N. Prasad, Proc. Natl. Acad. Sci. U.S.A. 102 (2005) 279.
[4] Y. Liu, H. Miyoshi, M. Nakamura, Colloids Surf. B: Biointerfaces 58 (2007) 180.
[5] Z.Z. Li, L.X. Wen, L. Shao, J.F. Chen, J. Control. Release 98 (2004) 245.
[6] S. Kim, T.Y. Ohulchansky, H.E. Pudavar, R.K. Pandey, P.N. Prasad, J. Am. Chem. Soc. 129 (2007) 2669.
[7] B. Moulari, D. Pertuit, Y. Pellequer, A. Lamprecht, Biomaterials 29 (2008) 4554.
[8] J. Swarbrick, J.C. Boylan, Encyclopedia of Pharmaceutical Technology, Informa Health Care, 2002.
[9] A. Rolland, Advanced Gene Delivery: From Concepts to Pharmaceutical Products, Harwood, Amsterdam, 1999.
[10] J. Panyam, W.Z. Zhou, S. Prabha, S.K. Sahoo, V. Labhasetwar, FASEB J. 16 (2002) 1217.
[11] Y.N. Konan, J. Chevallier, R. Gurny, E. Allémann, Photochem. Photobiol. 77 (2003) 638.
[12] Z.P. Xu, Q.H. Zeng, G.Q. Lu, A.B. Yu, Chem. Eng. Sci. 61 (2006) 1027.
[13] V. Escriou, M. CarriTre, D. Scherman, P. Wils, Adv. Drug Deliv. Rev. 55 (2003) 295.
[14] A.G. Tkachenko, H. Xie, D. Coleman, W. Glomm, J. Ryan, M.F. Anderson, S. Franzen, D.L. Feldheim, J. Am. Chem. Soc. 125 (2003) 4700.
[15] E. Katz, I. Willner, Angew. Chem. Int. Ed. 43 (2004) 6042.
[16] B.D. Chithrani, W.C.W. Chan, Nano Lett. 7 (2007) 1542.
[17] J.A. Champion, S. Mitragotri, Proc. Natl. Acad. Sci. U.S.A. 103 (2006) 4930.
[18] M.R. Lorenz, V. Holzapfel, A. Musyanovych, K. Nothelfer, P. Walther, H. Frank, K. Landfester, H. Schrezenmeier, V. Mailänder, Biomaterials 27 (2006) 2820.
[19] T.H. Chung, S.H. Wu, M. Yao, C.W. Lu, Y.S. Lin, Y. Hung, C.Y. Mou, Y.C. Chen, D.M. Huang, Biomaterials 28 (2007) 2959.
[20] D.J. Bharali, D.W. Lucey, H. Jayakumar, H.E. Pudavar, P.N. Prasad, J. Am. Chem. Soc. 127 (2005) 11364.
[21] M. Mäe, Ü. Langel, Curr. Opin. Pharm. 6 (2006) 509.
[22] H. Brooks, B. Lebleu, E. Vivès, Adv. Drug Deliv. Rev. 57 (2005) 559.
[23] E.P. Loret, E. Vives, P.S. Ho, H. Rochat, J. Van Rietschoten, W.C. Johnson Jr., Biochemistry 30 (1991) 6013.

[24] S. Ruben, A. Perkins, R. Purcell, K. Joung, R. Sia, R. Burghoff, W.A. Haseltine, C.A. Rosen, J. Virol. 63 (1989) 1.
[25] S. Fawell, J. Seery, Y. Daikh, C. Moore, L.L. Chen, B. Pepinsky, J. Barsoum, Proc. Natl. Acad. Sci. U.S.A. 91 (1994) 664.
[26] E. Vives, P. Brodin, B. Lebleu, J. Biol. Chem. 272 (1997) 16010.
[27] S. Futaki, T. Suzuki, W. Ohashi, T. Yagami, S. Tanaka, K. Ueda, Y. Sugiura, J. Biol. Chem. 276 (2001) 5836.
[28] A. Ziegler, P. Nervi, M. Dürrenberger, J. Seelig, Biochemistry 44 (2005) 138.
[29] A. Nori, K.D. Jensen, M. Tijerina, P. Kopeckova, J. Kopecek, J. Control. Release 91 (2003) 53.
[30] M. Paschke, W. Hohne, Gene 350 (2005) 79.
[31] L. Hyndman, J.L. Lemoine, L. Huang, D.J. Porteous, A.C. Boyd, X. Nan, J. Control. Release 99 (2004) 435.
[32] V.A. Sethuraman, Y.H. Bae, J. Control. Release 118 (2007) 216.
[33] S. Santra, H. Yang, D. Dutta, J.T. Stanley, P.H. Holloway, W. Tan, B.M. Mouldgil, R.A. Mericle, Chem. Commun. (2004) 2810.
[34] W.J. Tong, C.Y. Gao, J. Mater. Chem. 18 (2008) 3799.
[35] B.B. Jiang, L. Hu, C.Y. Gao, J.C. Shen, Int. J. Pharm. 304 (2005) 220.
[36] M.M. Fretz, E. Mastrobattista, G.A. Koning, W. Jiskoot, G. Storm, Int. J. Pharm. 298 (2005) 305.
[37] N.A.M. Verhaegh, A. Van Blaaderen, Langmuir 10 (1994) 1427.
[38] A. Van Blaaderen, V. Vrij, Langmuir 8 (1992) 2921.
[39] R.P. Bagwe, C. Yang, L.R. Hilliard, W. Tan, Langmuir 20 (2004) 8336.
[40] T.J. Yoon, K.N. Yu, E. Kim, J.S. Kim, B.G. Kim, S.H. Yun, B.H. Sohn, M.H. Cho, J.K. Lee, S.B. Park, Small 2 (2006) 209.
[41] Z.W. Ma, Z.W. Mao, C.Y. Gao, Colloids Surf. B: Biointerfaces 60 (2007) 137.
[42] Z.W. Mao, L. Ma, J. Zhou, C.Y. Gao, J.C. Shen, Bioconjug. Chem. 16 (2005) 1316.
[43] D. Lechardeur, A.S. Verkman, G.L. Lukacus, Adv. Drug Deliv. Rev. 57 (2005) 755.
[44] E. Vives, J.P. Richard, C. Rispal, B. Lebleu, Curr. Protein Pept. Sci. 4 (2003) 125.
[45] J.S. Wadia, R.V. Stan, S.F. Dowdy, Nat. Med. 10 (2004) 310.
[46] P.R. Leroueil, S.A. Berry, K. Duthie, G. Han, V.M. Rotello, D.Q. McNerny, J.R. Baker, B.G. Orr, M.M. Banaszak Holl, Nano Lett. 8 (2008) 420.
[47] M. Lindgren, M. Hallbrink, A. Prochiantz, U. Langel, Trends Pharmacol. Sci. 21 (2000) 99.
[48] M. Chen, A. von Mikecz, Exp. Cell. Res. 305 (2005) 51.